

RESEARCH

Pinning of dislocations in disordered alloys: Effects of dislocation orientation

Michael Zaiser^{1*} and Ronghai Wu²

*Correspondence:

michael.zaiser@fau.de¹Department of Materials Simulation, WW8-Materials Simulation, Friedrich-Alexander Universität Erlangen-Nürnberg, Dr.-Mack-str. 77, 90762 Fürth, Germany

Full list of author information is available at the end of the article

Abstract

The current interest in compositionally complex alloys including so called high entropy alloys has caused renewed interest in the general problem of solute hardening. It has been suggested that this problem can be addressed by treating the alloy as an effective medium containing a random distribution of dilatation and compression centers representing the volumetric misfit of atoms of different species. The mean square stresses arising from such a random distribution can be calculated analytically, their spatial correlations are strongly anisotropic and exhibit long-range tails with third-order power law decay [1, 2]. Here we discuss implications of the anisotropic and long-range nature of the correlation functions for the pinning of dislocations of arbitrary orientation. While edge dislocations are found to follow the standard pinning paradigm, for dislocations of near screw orientation we demonstrate the co-existence of two types of pinning energy minima.

Keywords: Compositionally complex alloys; Dislocations; Stacking fault; Critical resolved shear stress

1 Introduction

The theory of dislocations interacting with atomic-scale obstacles, traditionally formulated in the context of solution hardening, has seen a renaissance in recent years which has been driven by the general interest in compositionally complex alloy systems including so-called high-entropy alloys. In such alloys, multiple atomic species are present in comparable concentrations and entropic effects may stabilize homogeneous phases at elevated temperatures, whereas kinetic effects (slow diffusion due to multiple barriers and traps) may stabilize those phases against unmixing at reduced temperatures.

From a theoretical viewpoint, statistical theories of dislocation pinning by atomic-scale obstacles have, starting from the seminal work of Labusch [3, 4], attracted the interest of statistical physicists, and concepts developed for the pinning of elastic manifolds by random fields (e.g. [5]) and their depinning by external forces were applied to the athermal motion of dislocations (e.g. [6, 7]) and to dislocation motion at finite temperatures [8, 9]. In recent years, these concepts have been extended and adopted to compositionally complex and high entropy alloys by a number of authors (e.g. [10, 11, 12, 13, 14]). In particular, the group of W. Curtin has demonstrated that pinning of dislocations in compositionally complex alloys and the associated flow stress increase can to a large extent be explained in terms of the significant

local stress fluctuations introduced by the superposition of misfit strains associated with atomic species of significantly different atomic radius. Recently, [1, 2] evaluated the magnitude and spatial correlations of such random stress/strain fields. Here we use their result to study the effects of dislocation orientation on dislocation pinning by volumetric misfit fluctuations.

2 Scaling theory of elastic lines in static random fields

We envisage the dislocation as an elastic line of line tension $\mathcal{T} = \beta_0 \mu b^2$ where μ is the shear modulus, b the length of the Burgers vector, and the numerical parameter β_0 which is of the order of 1 may depend logarithmically on geometrical parameters characterizing the line shape. The dislocation is assumed macroscopically straight while local fluctuations of the line shape are described by a function $y(x)$ where the x axis is oriented along the average line direction and the y axis in perpendicular direction within the glide plane. Note that we assume $y(x)$ to be single valued, which excludes the presence of overhangs.

Let atomic disorder create a spatially fluctuating but temporally fixed resolved shear stress field $\tau(x, y)$ that acts on the dislocation, which is in addition subject to a spatially constant resolved shear stress τ_{ext} . The evolution of the dislocation line shape is then given by the quenched Edwards-Wilkinson equation

$$B \frac{dy}{dt} = \mathcal{T} \frac{\partial^2 y}{\partial x^2} + b[\tau(x, y) + \tau_{\text{ext}}] \quad (1)$$

The random shear stress $\tau(x, y)$ has the correlation function

$$\langle \tau(x, y) \tau(x', y') \rangle = \langle \tau^2 \rangle \Phi \left(\frac{|x - x'|}{a}, \frac{|y - y'|}{a} \right). \quad (2)$$

For a random alloy, the magnitude $\langle \tau^2 \rangle$ can be related to the average of the squared atomic misfit (see below) [1]. Analytical expressions that allow to compute the correlation function Φ have been given in Ref. [2] where the length scale parameter a was, by comparison with MD results, determined to be of the order of 1 \AA . For later use we introduce the notations $\Phi_{\perp}(y) := \Phi(x = 0, y)$ for the correlation function in the line-perpendicular and $\Phi_{\parallel}(x) := \Phi(x, y = 0)$ for the correlation function in the line-parallel direction.

We now evaluate the work per unit length done by the fluctuating stress as an infinitesimal dislocation segment at $(x, 0)$ displaces from $y = 0$ to $y = w$. This is given by $b \int_0^w \tau(x, y) dy$. We express the average value of this integral in terms of the conditional average of $\tau(x, y)$ given the stress at $(x, 0)$, i.e., $\langle \tau(x, y) \rangle_{\tau(x, 0)} = \tau(x, 0) \Phi_{\perp}(y/a)$: $\langle W_{\tau}(x, w) \rangle_{\tau(x, 0)} = b \tau(x, 0) \int_0^w \Phi_{\perp}(y/a) dy$.

Next we consider a segment of finite length L which is displaced by a distance w in the direction of the (mean) fluctuating stress τ acting on that segment, and we evaluate the mean square work:

$$\langle W_{\tau}^2 \rangle_{L, w} = \left\langle \left(\frac{1}{L} \int_0^L \langle \Delta E(x, w) \rangle_{\tau(x, 0)}^2 dx \right)^2 \right\rangle = \langle \tau^2 \rangle_L b^2 \left(\int_0^w \Phi_{\perp}(y/a) dy \right)^2 \quad (3)$$

This expression contains the average of the square fluctuating stress over the length L . The result is given by (see Appendix):

$$\langle \tau^2 \rangle_L = \langle \tau^2 \rangle \frac{1}{L} \int_{-L/2}^{L/2} \Phi_{\parallel} \left(\frac{x-x'}{a} \right) dx = \langle \tau^2 \rangle \frac{\xi - r(L)}{L} \quad (4)$$

where $\xi = \int_{-\infty}^{\infty} \Phi_{\parallel}(x/a) dx = \beta_1 a$ and $r(L) = 2 \int_{L/2}^{\infty} \Phi_{\parallel}(x/a) dx$. For sufficiently localized correlation functions one can, for $L \gg \xi$, neglect the residual $r(L)$. One then recovers the result for δ -correlated fluctuations where $\Phi_{\parallel}(x) = \xi \delta(x)$. We make this approximation in the following unless otherwise stated.

Under the fluctuating stress, segments move to reduce their energy. The characteristic energy reduction for a segment of length L moving over the distance w can be estimated as $E_{\text{RF}}(L, w) \approx \sqrt{\langle W_{\tau}^2 \rangle_{L,w}}$. To maintain connectivity between adjacent segments (which in general displace in different directions), the dislocation has to elongate. We estimate the corresponding energy cost by the energy per unit length of a triangular bulge of total width L and amplitude w :

$$E_{\text{LT}}(L, w) \approx \frac{2\mathcal{T}w^2}{L^2} \quad (5)$$

The total energy change per unit line length for segments of length L that displace independently to minimize their energy is then estimated as

$$\Delta E(L, w) = E_{\text{LT}}(L, w) - E_{\text{RF}}(L, w) \approx \frac{2\mathcal{T}w^2}{L^2} - b \left(\langle \tau^2 \rangle \frac{\xi}{L} \right)^{1/2} \int_0^w \Phi_{\perp}(y/a) dy \quad (6)$$

The pinning energy per unit length derives by minimizing this expression with respect to L and w . Setting $\partial_w \Delta E(L, w) = \partial_L \Delta E(L, w) = 0$ gives

$$\begin{aligned} 0 &= -4 \frac{\mathcal{T}w_p^2}{L_p^3} + \frac{b}{2} \sqrt{\langle \tau^2 \rangle \frac{\xi}{L_p^3}} \int_0^{w_p} \Phi_{\perp}(y/a) dy \\ 0 &= 4 \frac{\mathcal{T}w_p}{L_p^2} - b \sqrt{\langle \tau^2 \rangle \frac{\xi}{L}} \Phi_{\perp}(w_p/a) \end{aligned} \quad (7)$$

Both equations can be combined to eliminate the dislocation related parameters (\mathcal{T}, b, L) . It follows that the optimal displacement depends only on properties of the correlation function and obeys the equation:

$$2w_p \Phi_{\perp}(w_p/a) = \int_0^{w_p} \Phi_{\perp}(x/a) dx \quad (8)$$

We may now use these results to obtain from Eq. (7) the pinning length L_p . With the notations $\xi = \beta_1 a$, $w_p = \beta_2 a$ we get

$$L_p = \left(\frac{16\beta_2^2}{\beta_1 \Phi_{\perp}^2(w_p/a)} \right)^{1/3} \left(\frac{\mathcal{T}}{\sqrt{\langle \tau^2 \rangle} b} \right)^{2/3} a^{1/3} \quad (9)$$

Setting finally $\mathcal{T} = \beta_0 \mu b^2$ we find the scaling relation

$$L_p = \left(\frac{16\beta_1^2\beta_2^2\beta_0^2}{\beta_1\Phi_\perp^2(w_p/a)} \right)^{1/3} \left(\frac{\mu}{\sqrt{\langle\tau^2\rangle}} \right)^{2/3} b^{2/3} a^{1/3} = C_L \left(\frac{\mu}{\sqrt{\langle\tau^2\rangle}} \right)^{2/3} b^{2/3} a^{1/3} \quad (10)$$

Inserting (10) into (6) gives the pinning energy which results as:

$$E_p = -3 \left(\frac{\beta_1^2\beta_2^2\Phi_\perp^4(w_p/a)}{4\beta_0} \right)^{1/3} \frac{\sqrt{\langle\tau^2\rangle}^{4/3}}{\mu^{1/3}} a^{4/3} b^{2/3} = C_E \frac{\sqrt{\langle\tau^2\rangle}^{4/3}}{\mu^{1/3}} a^{4/3} b^{2/3} \quad (11)$$

Finally, the critical shear stress is estimated by equating the pinning energy to the work done by the external shear stress in moving the dislocation over the pinning displacement w_p :

$$\tau_{\text{ext,c}} = \frac{E_p}{bw_p} = C_\tau \frac{\sqrt{\langle\tau^2\rangle}^{4/3}}{\mu^{1/3}} \left(\frac{a}{b} \right)^{1/3}. \quad (12)$$

3 Application to dislocation pinning in random alloys

3.1 Statistical properties of local shear stresses: A compilation of results

For an alloy constituting a random distribution of different atomic species which depending on atomic radius act as dilatation or compression centers in the effective medium of the alloy, statistical properties of the ensuing shear stress field were calculated by Geslin et. al. [1, 2]. In this paragraph we summarize their results. The mean square shear stress in an arbitrary plane is given by

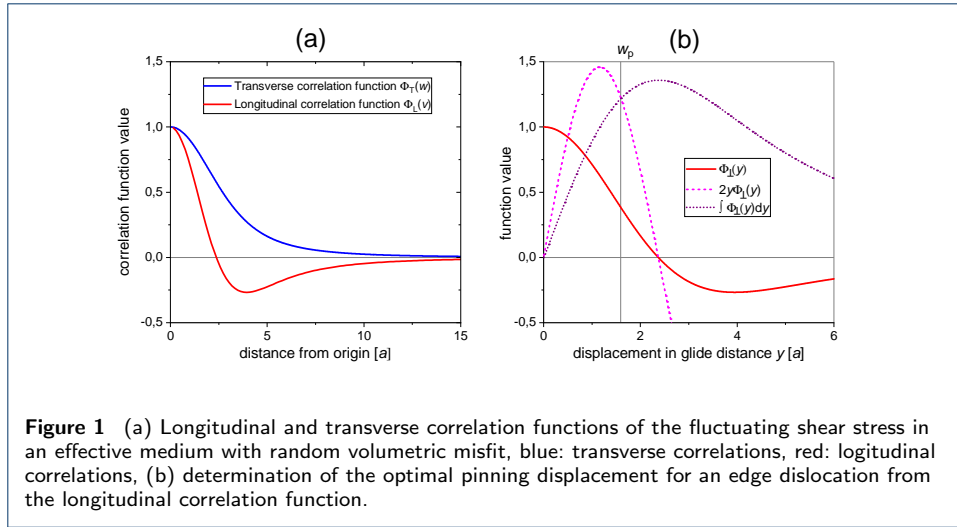
$$\langle\tau^2\rangle = \frac{V_a \langle\Delta\epsilon^2\rangle \mu}{30\pi^{3/2} a^3} \quad (13)$$

where V_a is the atomic volume, $\langle\Delta\epsilon^2\rangle$ is the mean square volumetric strain (dilatation or compression) introduced by an individual atom into the effective medium constituted by the random alloy. The characteristic length a arises in the treatment of Geslin et. al. as a regularization length that characterizes the distribution of the volumetric strain around the atom position. By comparison of theoretical results with stresses determined from molecular statics simulations, this parameter was determined by Geslin et. al. for different alloys and found to be close to $a = 1\text{\AA}$.

The correlation functions in the shear direction ('longitudinal' correlation function Ψ_L) and in perpendicular direction in the shear plane ('longitudinal' correlation function Ψ_T) are derived by Geslin et. al. as

$$\begin{aligned} \Psi_L(u) &= -\frac{30}{u^3} \left[\sqrt{\pi} \left(1 - \frac{12}{u^2} \right) \operatorname{erf} \left(\frac{u}{2} \right) + \frac{1}{u} (12 + u^2) \exp \left(-\frac{u^2}{4} \right) \right], \\ \Psi_T(u) &= \frac{15}{u^3} \left[\sqrt{\pi} \left(1 - \frac{6}{u^2} \right) \operatorname{erf} \left(\frac{u}{2} \right) + \frac{6}{u} \exp \left(-\frac{u^2}{4} \right) \right], \end{aligned} \quad (14)$$

where $u = d/a$ and d denotes the distance from the origin in the respective direction. The correlation functions are plotted in Figure 1 which shows the anisotropic nature



of the correlations. The corresponding correlation integrals, which are needed to evaluate pinning parameters, are given by

$$\begin{aligned} \int_0^U \Psi_L(u) du &= \frac{15}{U^4} \left[\sqrt{\pi} (U^2 - 6) \operatorname{erf} \left(\frac{U}{2} \right) + 6 \exp \left(-\frac{U^2}{4} \right) \right], \\ \int_0^U \Psi_T(u) du &= \frac{15}{8U^4} \left[\sqrt{\pi} (U^4 - 4U^2 + 12) \operatorname{erf} \left(\frac{U}{2} \right) + (2U^3 - 12U) \exp \left(-\frac{U^2}{4} \right) \right], \end{aligned} \quad (15)$$

The correlation function in an arbitrary direction that makes an angle θ with the shearing direction is found to be

$$\Psi(\theta, u) = \Psi_L(u) \cos^2 \theta + \Psi_T(u) \sin^2 \theta \quad (16)$$

and the corresponding correlation integrals derive by analogous superposition of the integrals in Eq. (15).

3.2 Pinning of an edge dislocation

We consider a perfect edge dislocation where the shear direction (the direction of the Burgers vector) is perpendicular to the dislocation line. We can thus identify the x coordinate of the dislocation coordinate system with the transverse coordinate, $\Psi_T(u) = \Phi_{\parallel}(x/a)$ and the y coordinate with the longitudinal coordinate, $\Psi_L = \Phi_{\perp}(y/a)$. The correlation length ξ is evaluated as the integral of the parallel correlation function over the x axis. From Eq. (15) it follows that

$$\xi = \int_{-\infty}^{\infty} \Phi_{\parallel}(x/a) dx = \frac{15\sqrt{\pi}}{4} a \approx 6.6a. \quad (17)$$

Hence, the correlation length parameter $\beta_1 \approx 6.6$. In a simplified scaling analysis we neglect the residual that remains when the integral is restricted to the interval $|x| \leq L/2$. For $L \gg \xi$ this residual can be evaluated from the asymptotic behavior

Table 1 Parameters used in numerical calculations.

Parameter	Unit	Numerical value
shear modulus μ	GPa	20.7
Burgers vector length b	Å	3.05
solute core parameter a	Å	1.0
mean square shear stress $\langle\tau^2\rangle$	GPa ²	0.6
line tension parameter $\beta_0^e = \mathcal{T}_e/(\mu b^2)$	–	0.35
line tension parameter $\beta_0^s = \mathcal{T}_s/(\mu b^2)$	–	1.05

of the correlation function as

$$r = -2 \int_{L/2}^{\infty} \Phi_{\parallel}(x/a) dx \approx -30\sqrt{\pi} \int_{L/2}^{\infty} \left(\frac{a}{x}\right)^3 dx = 60\sqrt{\pi}a \left(\frac{a}{L}\right)^2. \quad (18)$$

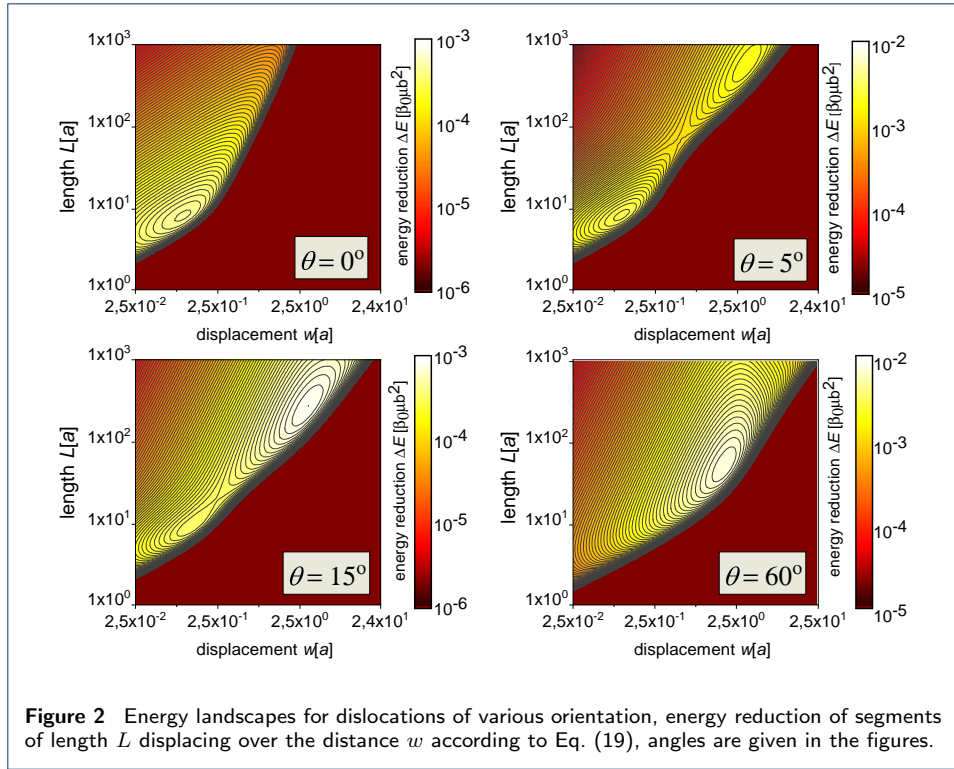
which provides, once the pinning length is determined, a simple check of the accuracy of the approximation $r \ll \xi$

We now use Eq. (8) to determine the optimum pinning displacement $w_p =$ from the longitudinal correlation function Φ_{\perp} as shown in Figure 1, (b). We find that $w_p = 1.59a$, hence $\beta_2 = 1.59$, and $\Phi_{\perp}(w_p/a) = 0.38$.

As a numerical example we consider a hypothetical $\text{Al}_{0.5}\text{Mg}_{0.5}$ fcc random solid solution for which simulations reported in Ref. [2] give the values $\mu = 20.7$ GPa, $a \approx 1\text{Å}$, and $\langle\tau^2\rangle = 0.6$ GPa². For the Burgers vector length we use a value of 3.02Å , which is the arithmetic mean of the Burgers vector length in Al and the a lattice spacing in Mg. For the line tension associated with the bow out of an edge dislocation, we refer to Ref. [15] who determine, from thermal vibrations of an edge dislocation line, an effective line tension of $\mathcal{T} \approx 0.35\mu b^2$, hence $\beta_0^e = 0.35$. For a screw dislocation we consider a pre-factor $\beta_0^s \approx 2.5\beta_0^e$. While isotropic elasticity theory predicts higher values, both experimental investigations [16] and recent atomistic simulations [17] suggest for fcc crystals a ratio $\beta_0^s/\beta_0^e \approx 2 \dots 2.5$, so using a ratio of 3 may serve as an acceptable compromise. More accurate and material specific values can, if needed, be deduced from molecular dynamics simulations of the thermal roughening of dislocation lines, using the method described in Ref. [15]. All parameters we used in our numerical examples are compiled in Table 1.

With these parameters we obtain for a pure edge dislocation $L_p = 32.9 \text{Å} \gg \xi = 6.18 \text{Å}$. Eq. (11) gives for the pinning energy per unit length $E_p \approx 1,83 \times 10^{-11} \text{J/m} \approx 0.01\mu b^2$, and the critical resolved shear stress derives from Eq. (12) as $\tau_{\text{ext,c}} = 390 \text{MPa}$.

With the pinning length given above we can estimate the residual $r(L_p)$ which with Eq. (17) follows as $r(L_p) = 0.106$. This demonstrates that the approximation made in neglecting this residual is acceptable. We note that, in scaling analysis of pinning problems, this approximation is often postulated *a priori* by approximating the correlation function in the line parallel direction as $\Phi_{\parallel}(x) = \xi\delta(x)$. The fact that we obtain, up to minor corrections, the same result as for such uncorrelated disorder demonstrates that an asymptotic third-order decay of the correlator, contrary to the conjecture of Ref. [2], not necessarily violates the assumption of short-range correlations used in standard scaling arguments. However, as we shall see, the case of a perfect screw dislocation illustrates how standard scaling arguments can go wrong.



3.3 Pinning of a screw dislocation

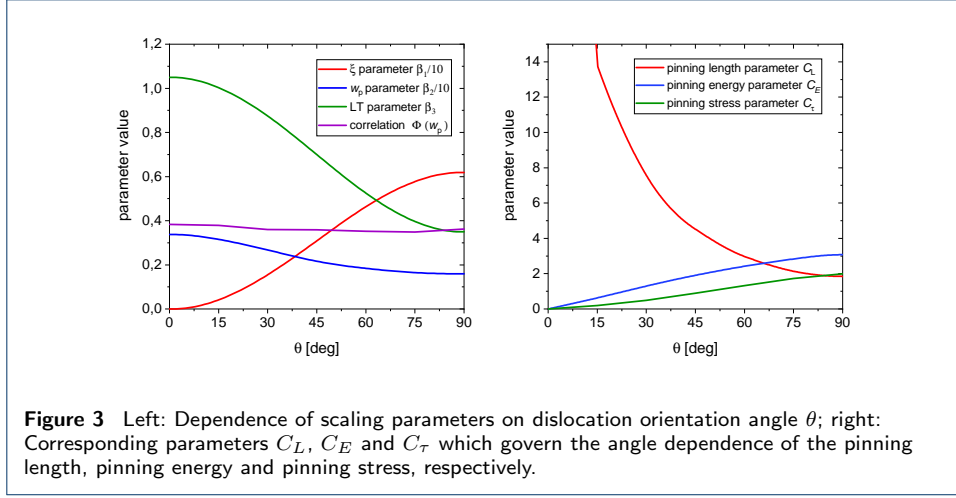
If the dislocation orientation has screw orientation, the above treatment becomes spurious because the correlation function Φ_{\parallel} for a screw dislocation integrates to zero, the corresponding pinning length would therefore diverge and accordingly the pinning energy and pinning stress would be zero. For a screw dislocation we therefore investigate the energy gain $\Delta E(w, L)$ using the full expressions for the integral over Φ_{\parallel} that arises when averaging the fluctuating stress over a segment of length L :

$$\Delta E(L, w) \approx \frac{2\beta_0\mu b^2 w^2}{L^2} - b \left(\langle \tau^2 \rangle \frac{1}{L} \int_{-L/2}^{L/2} \Phi_{\parallel}(x/a) dx \right)^{1/2} \int_0^w \Phi_{\perp}(y/a) dy \quad (19)$$

The corresponding energy landscape is illustrated in Figure 2, top left. There is an energy minimum located at $L \approx 6a$, in good agreement with the range over which the correlation function Ψ_L , i.e. the line parallel correlation function for screw dislocations, is positive. However, the corresponding optimal displacement $w \approx 0.08a$ is tiny and accordingly the maximum energy gain is small, amounting to $\Delta E_{p,s} = 0.054 \times 10^{-11} \text{ J/m} = 2.85 \times 10^{-4} \mu b^2$. Nevertheless, because of the smallness of w_p Eq. (12) predicts a significant pinning stress of about 190 MPa, half the value for the edge dislocation.

3.4 Pinning of a general dislocation

For a dislocation of general orientation θ where θ is the angle between the line direction and the Burgers vector, it follows from Eq. (15) that the line-parallel and



line-perpendicular correlation functions are

$$\begin{aligned}\Phi_{\parallel}(u) &= \Psi_L(u) \cos^2 \theta + \Psi_T(u) \sin^2 \theta, \\ \Phi_{\perp}(u) &= \Psi_L(u) \sin^2 \theta + \Psi_T(u) \cos^2 \theta.\end{aligned}\quad (20)$$

Moreover, we assume that the line tension varies with the angle θ according to $\mathcal{T}(\theta) = \beta_0(\theta)\mu b^2$ where, for simplicity, we consider a simple sinusoidal variation:

$$\beta_0 = \beta_0^s \cos^2 \theta + \beta_0^e \sin^2 \theta \quad (21)$$

This allows us to study the angle dependence of the pinning parameters.

3.4.1 Edge-like pinning

We first use a simplified treatment which, as in case of an edge dislocation, neglects the correlation residual $r(L)$. We thus base our analysis upon Eqs. (6-12). Since the longitudinal correlation function Φ_L integrates to zero, the correlation length parameter is, upon neglecting the residual integral $r(L)$, given by

$$\beta_1 = \beta_1^e \sin^2 \theta. \quad (22)$$

Finally, we numerically establish the orientation dependence of the optimum pinning displacement $w_p(\theta)$ and the corresponding function value $\Psi_{\perp}(w_p(\theta))$ using Eq. (8).

All θ dependent parameters are compiled in Figure 3, left. From these parameters we can compute the angle dependent parameters C_L , C_E and C_θ . The respective physical variables are obtained from these by multiplication with material and fluctuation parameters according to Eqs. (10)-(12). The parameter C_L increases as we move away from the edge orientation, whereas the correlation length parameter β_1 decreases. Accordingly, our analysis, which is built upon the smallness of ξ/L and a/L , becomes more accurate. We denote this behavior as edge-like pinning. The corresponding energy landscape is illustrated in Figure 2, bottom right, for the case of a 60 deg dislocation.

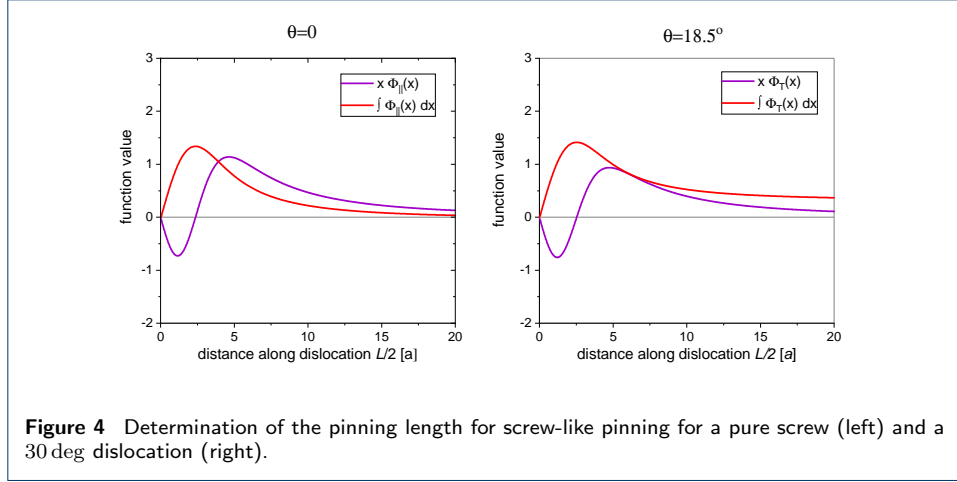


Figure 4 Determination of the pinning length for screw-like pinning for a pure screw (left) and a 30 deg dislocation (right).

In the screw dislocation limit our analysis however implies a diverging pinning length and vanishing pinning stress and energy, at variance with the findings of section 3.3. In fact, the energy minimum seen in Figure 2, top left, for the screw dislocation actually represents a different class of 'screw-like' pinning behavior which we now investigate.

3.4.2 Screw-like pinning

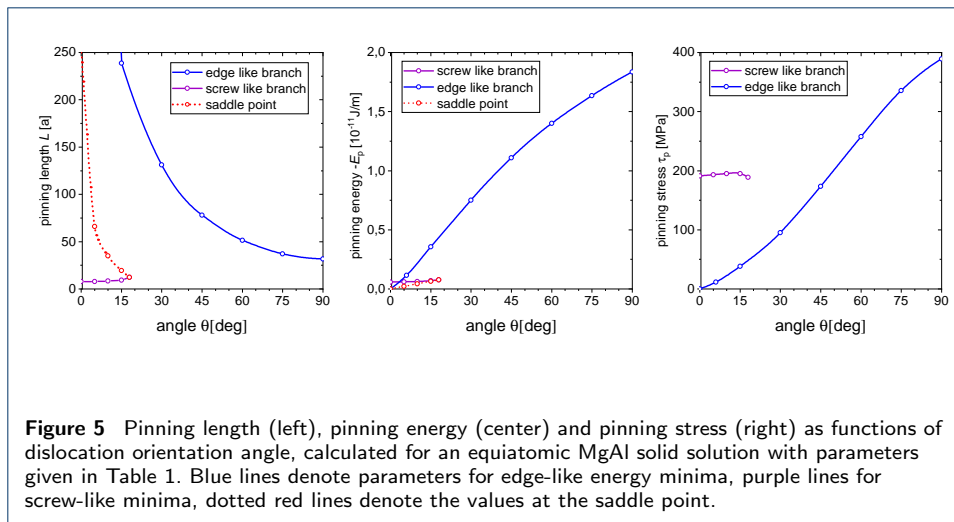
We base our analysis upon Eq. (19) which we simplify using the observation that, in case of screw dislocation pinning, the pinning displacement w_p which optimizes the energy gain is very small. Accordingly, we can approximate $\int_0^w \Phi_{\parallel}(x/a)dx \approx w$. The extremum condition $\partial_w \Delta E(L, w) = \partial_L \Delta E(L, w) = 0$ then gives

$$\begin{aligned}
 0 &= 4 \frac{\mathcal{T} w_p}{L_p^2} - b \sqrt{\langle \tau^2 \rangle} \left(\frac{\int_{-L_p/2}^{L_p/2} \Phi_{\parallel}(x/a) dx}{L_p} \right)^{1/2} \\
 0 &= -4 \frac{\mathcal{T} w_p^2}{L_p^3} - b \frac{\sqrt{\langle \tau^2 \rangle} w_p}{2L_p} \left(\frac{L_p \Phi_{\parallel}(L_p/2a)}{\left[\int_{-L_p/2}^{L_p/2} \Phi_{\parallel}(x/a) dx \right]^{1/2}} - \left[\frac{\int_{-L_p/2}^{L_p/2} \Phi_{\parallel}(x/a) dx}{L_p} \right]^{1/2} \right)
 \end{aligned} \tag{23}$$

Both equations can again be combined to eliminate the dislocation related parameters (\mathcal{T}, b, L) , which produces an equation for the pinning length:

$$-\frac{L_p}{2a} \Phi_{\parallel}(L_p/2a) = \int_0^{L_p/2} \Phi_{\parallel}(x/a) dx. \tag{24}$$

The situation is illustrated in Figure 4 for the cases of a pure screw ($\theta = 0$) and a 15 deg dislocation. In this range, the equation has two solutions, corresponding to a minimum and a saddle point of the energy surface. The two solutions merge at an angle slightly above $\theta = 18$ deg, so there are no screw-like solutions for larger angles. At the same time, the saddle point moves to $L \rightarrow \infty$ as $\theta \rightarrow 0$ and thus merges with the edge-like minimum. The resulting energy landscapes are characterized by a



ridge with two peaks (maxima of the energy reduction as the dislocation adjusts to the pinning landscape) and a saddle point. Such energy landscapes are illustrated in Figure 2, top right and bottom left, for angles $\theta = 5$ deg and $\theta = 15$ deg.

3.4.3 Numerical example

We now apply the previously obtained relations to the case of the $\text{Mg}_{0.5}\text{Al}_{0.5}$ alloy studied by Geslin et. al. [2]. We calculate pinning length, pinning energy and pinning stress for orientations between 0 and 90 deg using the relations for edge-like pinning (large pinning length, significant pinning displacement), and for orientations between 0 and 30 degrees, where the screw-like energy minimum exists, we compute the same parameters also for screw-like pinning. For the pinning length, we also show the unstable saddle point.

Parameters are found in Table 1, and results are compiled in Figure 5. For near screw orientations the results show a co-existence of two pinning branches which show an interesting dichotomy, as the edge-like branch (except very close to the pure screw orientation) is characterized by an energy minimum that is deeper but much less steep, leading to a reduced pinning stress. The screw like branch, on the other hand, shows small pinning energies but, because the small pinning displacements lead to a steep slope of the energy landscape, appreciable pinning stresses. Which of these minima dominates the plastic behavior is difficult to decide without consideration of thermal activation and history effects.

4 Discussion and Conclusions

Our calculations demonstrate that, in addition to well known line tension effects which lead to reduced pinning of screw relative to edge dislocations, the anisotropy of shear stresses created by an assembly of compression/dilatation centers has a major influence on the anisotropic pinning of dislocations. Edge dislocations and near edge dislocations follow the standard pinning paradigm despite a third law power decay of the stress correlator. Pinning of screw and near screw dislocations, on the other hand, is characterized by a different type of energy minimum with

much reduced pinning length and pinning displacement. Pinning stresses of near-screw dislocations are slightly lower than those of edge dislocations, but more importantly, the depth of the energy minimum for screw-like pinning is much lower than for edge-like pinning. As a consequence, at elevated temperature the motion of edge dislocations, being controlled by deep energy minima, is expected to be much more difficult than the motion of screw dislocations. This may serve as a generic explanation for recently reported observations in bcc High Entropy alloys [18].

While we have established generic relationships that allow to separate the effects of line tension and of statistical parameters of the fluctuating stress field, in present form these relationships are applicable to perfect dislocations only. In High Entropy alloys, where stacking fault energies may be low, wide core splitting of dislocations introduces an additional degree of freedom which needs to be taken into account in pinning theories. Since the partials of a split dislocation have in general mixed character, we expect an even more complex energy landscape whose study we postpone to future work.

Declarations

Competing interests

The authors declare that they have no competing interests.

Author's contributions

MZ formulated the equations, R.W. performed numerical and analytical calculations, M.Z. drafted the manuscript which was edited and approved jointly by both authors.

Funding

M.Z. and R.W. acknowledge funding by DFG under Grant No. 1 Za 171/8-1.

Availability of data and material

Not applicable.

Author details

¹Department of Materials Simulation, WW8-Materials Simulation, Friedrich-Alexander Universität Erlangen-Nürnberg, Dr.-Mack-str. 77, 90762 Fürth, Germany. ²School of Mechanics, Civil Engineering and Architecture, Northwestern Polytechnical University 710129 Xian, P.R. China.

References

1. Geslin, P.-A., Rodney, D.: Microelasticity model of random alloys. part i: mean square displacements and stresses. *Journal of the Mechanics and Physics of Solids* **153**, 104479 (2021)
2. Geslin, P.-A., Rida, A., Rodney, D.: Microelasticity model of random alloys. part ii: displacement and stress correlations. *Journal of the Mechanics and Physics of Solids* **153**, 104480 (2021)
3. Labusch, R.: A statistical theory of solid solution hardening. *physica status solidi (b)* **41**(2), 659–669 (1970)
4. Labusch, R.: Statistische theorien der mischkristallhärtung. *Acta Metallurgica* **20**(7), 917–927 (1972)
5. Chauve, P., Giamarchi, T., Le Doussal, P.: Creep and depinning in disordered media. *Physical Review B* **62**(10), 6241 (2000)
6. Zapperi, S., Zaiser, M.: Depinning of a dislocation: the influence of long-range interactions. *Materials Science & Engineering A* **309**(2), 348–351 (2001)
7. Bakó, B., Weygand, D., Samaras, M., Hoffelner, W., Zaiser, M.: Dislocation depinning transition in a dispersion-strengthened steel. *Physical Review B* **78**(14), 144104 (2008)
8. Ioffe, L.B., Vinokur, V.M.: Dynamics of interfaces and dislocations in disordered media. *Journal of Physics C: Solid State Physics* **20**(36), 6149 (1987)
9. Zaiser, M.: Dislocation motion in a random solid solution. *Philosophical Magazine A* **82**(15), 2869–2883 (2002)
10. Toda-Caraballo, I., Rivera-Díaz-del-Castillo, P.E.: Modelling solid solution hardening in high entropy alloys. *Acta Materialia* **85**, 14–23 (2015)
11. Wu, Z., Gao, Y., Bei, H.: Thermal activation mechanisms and labusch-type strengthening analysis for a family of high-entropy and equiatomic solid-solution alloys. *Acta Materialia* **120**, 108–119 (2016)

12. Varvenne, C., Luque, A., Curtin, W.A.: Theory of strengthening in fcc high entropy alloys. *Acta Materialia* **118**, 164–176 (2016)
13. Varvenne, C., Leyson, G., Ghazisaeidi, M., Curtin, W.: Solute strengthening in random alloys. *Acta Materialia* **124**, 660–683 (2017)
14. LaRosa, C.R., Shih, M., Varvenne, C., Ghazisaeidi, M.: Solid solution strengthening theories of high-entropy alloys. *Materials Characterization* **151**, 310–317 (2019)
15. Zhai, J.-H., Zaiser, M.: Properties of dislocation lines in crystals with strong atomic-scale disorder. *Materials Science and Engineering: A* **740**, 285–294 (2019)
16. Mughrabi, H.: Self-consistent experimental determination of the dislocation line tension and long-range internal stresses in deformed copper crystals by analysis of dislocation curvatures. *Materials Science and Engineering: A* **309**, 237–245 (2001)
17. Szajewski, B., Pavia, F., Curtin, W.: Robust atomistic calculation of dislocation line tension. *Modelling and Simulation in Materials Science and Engineering* **23**(8), 085008 (2015)
18. Kubilay, R., Ghafarollahi, A., Maresca, F., Curtin, W.: High energy barriers for edge dislocation motion in body-centered cubic high entropy alloys. *npj Computational Materials* **7**(1), 1–9 (2021)

Appendix A: Mean shear stress fluctuation acting on a straight dislocation segment

The mean square fluctuations of the shear stress acting on a straight dislocation segment of length L located between the points $(-L/2, 0)$ and $(L/2, 0)$ depend on the transverse correlation function. They derive as

$$\begin{aligned} \langle \tau^2 \rangle_L &= \left\langle \left(\frac{1}{L} \int_{-L/2}^{L/2} \tau(x, 0) dx \right)^2 \right\rangle = \frac{1}{L^2} \iint_{-L/2}^{L/2} \langle \tau(x, 0) \tau(x', 0) \rangle dx dx' \\ &= \frac{\langle \tau^2 \rangle}{L^2} \iint_{-L/2}^{L/2} \Phi_{\parallel} \left(\frac{|x - x'|}{a} \right) dx dx' \end{aligned} \quad (25)$$

To evaluate the integral we introduce the notation $\tilde{x} = x - x'$:

$$\langle \tau^2 \rangle_L = \langle \tau^2 \rangle \frac{1}{L^2} \int_{-L/2}^{L/2} \int_{-L/2-\tilde{x}}^{L/2-\tilde{x}} \Phi_{\parallel}(|\tilde{x}|/a) d\tilde{x} dx \quad (26)$$

The inner integral can be re-written as

$$\begin{aligned} \int_{-L/2-\tilde{x}}^{L/2-\tilde{x}} \Phi_{\parallel}(\tilde{x}) d\tilde{x} &= \frac{1}{2} \left(\int_{-L/2-\tilde{x}}^{L/2-\tilde{x}} \Phi_{\parallel}(\tilde{x}) d\tilde{x} + \int_{-L/2+\tilde{x}}^{L/2+\tilde{x}} \Phi_{\parallel}(\tilde{x}) d\tilde{x} \right) \\ &= \int_{L/2}^{L/2} \Phi_{\parallel}(\tilde{x}) d\tilde{x} = \xi - r \quad , \quad r = 2 \int_{L/2}^{\infty} \Phi_{\parallel}(\tilde{x}) d\tilde{x}. \end{aligned} \quad (27)$$

where we have exploited the symmetry of the correlation function.